

## EXPERIMENTAL STUDY FOR STAGGERED PERFORATED ARRAY OF PINS LIKE FINS IN A RECTANGULAR AIR CROSS FLOW

Ali Shakir Baqir<sup>a</sup>, Ahmed Qasim<sup>b</sup>, Anmar Adnan<sup>b</sup>

<sup>a</sup> Najaf Technical College, Najaf, Iraq, [baqireng@yahoo.com](mailto:baqireng@yahoo.com), <sup>b</sup> Baghdad Technical College, Iraq, Dept. of Refrigeration and Air conditioning Eng.

### ABSTRACT

This paper investigated experimentally the friction factor reduction and heat transfer enhancement processes over staggered perforated pin fins in a rectangular channel with air cross flow. The channel had a duct cross section width of 62 mm, cross section depth of 167 mm and duct length of 1200 mm. The experiment covers the following ranges: Reynolds number 28000-113000, and pin fin shapes (solid, horizontal/vertical (HV) perforation and horizontal/vertical/lateral (HLV) perforation). Results show that the Nusselt numbers of pins with horizontal/vertical (HV) perforations are about 11% higher than those for solid pins and with horizontal /vertical/lateral (HLV) perforations are about 21% higher than those for the solid pins.. In addition, experimental results show that pins with horizontal/vertical/lateral (HLV) perforations, have good enhancement of heat transfer in addition to a significant reduction in weight compared with solid pin case performance.

**Keywords:** Perforated pin fins, Heat sink, Heat transfer enhancement, Thermal efficiency, Pressure drop, fin performance and thermal resistance.

### دراسة عملية لمجموعة متداخلة من قضبان مثقبة تشبه الزعانف في قناة مستطيلة المقطع يتدفق عبرها الهواء بشكل عمودي

الخلاصة:

يتقصى هذا البحث تجريبيا اجراءات تقليل معامل الاحتكاك وتعزيز انتقال الحرارة لمجموعة قضبان متداخلة مثقبة تشبه الزعانف في قناة مستطيلة المقطع يتدفق عبرها الهواء بشكل عمودي . عرض المقطع العرضي للقناة 62 ملم , عمق المقطع العرضي 167 ملم وطول المجرى الهوائي 1200 ملم . غطت التجربة النطاق التالي : عدد رينولدز , 28000-113000 ، شكل القضبان التي تشبه الزعانف المستخدمة في الجانب العملي هي قضبان صلبة تشبه الزعانف , قضبان تشبه الزعانف ذات ثقوب أفقية /عمودية وقضبان تشبه الزعانف ذات ثقوب افقية / جانبية / عمودية . خمنت النتائج على ان عدد نسلت للقضبان التي تشبه الزعانف ذات الثقوب الافقية /العمودية بحوالي 11% أعلى منه في القضبان الصلبة التي تشبه الزعانف وللقضبان التي تشبه الزعانف ذات الثقوب الافقية /الجانبية /العمودية بحوالي 21% اعلى منه في القضبان الصلبة التي تشبه الزعانف . أظهرت النتائج التجريبية بأن القضبان التي تشبه الزعانف ذات ثقوب افقية / جانبية / عمودية لديها تعزيز نقل الحرارة و كفاءة حرارية وفعالية للزعانف جيدة . علاوة على ذلك فهي تسبب انخفاض مؤثر في الوزن مقارنة بالقضبان الصلبة التي تشبه الزعانف.

## SYMBOLS

|           |   |
|-----------|---|
| $A_s$     | Heat transfer area (m <sup>2</sup> )          |
| $b$       | Test section base length and width (mm)       |
| $c$       | Clearance between the fin and duct (mm)       |
| $d_{hp}$  | Horizontal perforation diameter (mm)          |
| $d_{vp}$  | Vertical perforation diameter (mm)            |
| $d_{lp}$  | Lateral perforation diameter (mm)             |
| $d$       | Diameter of pin fins (mm)                     |
| $d_h$     | Hydraulic diameter of the duct (mm)           |
| $f$       | Friction factor                               |
| $h$       | Heat transfer coefficient, W/m <sup>2</sup> K |
| $H$       | Height of the pin fins (mm)                   |
| $K$       | Thermal conductivity (W/m K)                  |
| $l$       | Duct cross section depth (mm)                 |
| $L$       | Duct length (mm)                              |
| $N$       | Pin fins number                               |
| $N_p$     | Perforation number                            |
| $Nu$      | Nusselt number                                |
| $P$       | Pressure (kPa)                                |
| $Re$      | Reynolds number                               |
| $R_{tot}$ | Total thermal resistance °C/w                 |
| $S$       | Pitch (mm)                                    |
| $T$       | Temperature (°C)                              |
| $V$       | Average inlet velocity (m/s)                  |
| $w$       | Duct cross section width (mm)                 |

## Greek

|              |   |
|--------------|---|
| $\Delta P$   | Pressure difference (kPa)                           |
| $\epsilon_f$ | fin effectiveness                                   |
| $\eta$       | Thermal efficiency (Pa) <sup>-1</sup>               |
| $\rho_{air}$ | Density of air (kg m <sup>-3</sup> )                |
| $\mu_{air}$  | Viscosity of air kg m <sup>-1</sup> s <sup>-1</sup> |

## Subscripts

|          |   |
|----------|---|
| $av$     | average                                 |
| $b$      | Refer to the fin base                   |
| $HLV$    | Horizontal/lateral/vertical perforation |
| $HV$     | Horizontal/vertical perforation         |
| $in$     | inlet                                   |
| $m$      | Mean                                    |
| $out$    | outlet                                  |
| $s$      | Smooth                                  |
| $\infty$ | Free stream                             |

## INTRODUCTION:

A key challenge in the design of efficient heat sink systems, like the electronic components, is to achieve effectively the thermal energy generated with a minimum of material weight and cost. Therefore, various types of fins, such as pin, rectangular, square and annular perforated fins have been used in the efficient heat sink systems. There have been many experimental, theoretical and numerical investigations regarding heat transfer enhancement and pressure drop reduction in channels with in a heat sink system, which are limited to perforated pin fins. Foo et al. 2012 investigated numerically the use of staggered perforated pin fins to enhance the rate of heat transfer with impinging flow. They found that heat transfer increases with an increasing (i) number of perforations, (ii) horizontal perforation diameter, and (iii) coupling horizontal and vertical perforation diameters. In addition, the study showed that the pressure drop across the heat sink is smaller with increasing number of perforation and perforation diameter. Tahat et al. 2000 determined the optimal spacing of the fins in wise span and wise stream directions for staggered and inline arranged pin fins. Shaeri and Yaghoubi 2009 investigated numerically three-dimensional fluid flow and convection heat transfer from an array of solid and perforated fins that are mounted on a flat plate. The study showed that the total drag is highest when increasing number of perforations, the size of formed wake behind the fin decreased. In addition, they found that temperature drop from the fin base to fin top surface increases with additions of perforations. Bayram and Alparslan 2008 reported on heat transfer enhancement and corresponding pressure drop over a flat surface equipped with square cross-sectional perforated pin fins in a rectangular channel. Kai-Shaing et al. 2007 conducted a comparative study of pin fins sinks having circular, elliptic, and square cross-section. They tested and made twelve pin fin heat sinks having inline and staggered arrangements. Tzer and Sheng 2005 presented a novel semi-empirical model for estimating the permeability and inertia coefficient of pin fin heat sinks that are set as porous media. Sparrow et al. 1980 investigated experimentally the effects of staggered and inline pin fin arrays on thermal dissipation and pressure drop. They showed that convective heat transfer and pressure drop for staggered arrays are higher than those for the in-line arrays. Shaeri et al. 2009 studied numerically fluid flow and conjugate conduction-convective heat transfer from a three-dimensional he array of rectangular perforated fins with square windows that are arranged in lateral surface of fins. Diani et al. 2013 presented the numerical and experimental studies during turbulent air forced convection through extended surfaces. They used new models for the design of optimized heat sink configurations for a given electronic cooling application by comparing the heat transfer and fluid-dynamic different behaviors of plain and pin fin surfaces.

The aim of the present study is to investigate experimentally the effects of horizontal, lateral, and vertical perforations on the convective heat transfer and pressure drop for fin pin heat sink system. Of course, the parameters used in this study (5 horizontal perforations, 1 vertical perforations, and all of 3 mm in diameters) are similar to those in Foo et al. 2008, but in this study has been added to the effect of 5 lateral perforations with 3 mm diameters and all of them in air parallel flow channel.

## Equipment and Procedure:

The experimental insulated test rig (Edibon technical teaching equipment/TIFCC) was to study the effects of solid, horizontal/vertical, and lateral/horizontal/vertical perforation pin fins on the heat transfer enhancement and pressure drop (Fig. 1a, 1b). The duct channel length is of 1200 mm and cross section width 62 mm and cross section depth 167 mm. The test pin fin assembly was manufactured in Najaf Technical College laboratories. The test section base size, perforation size, duct, and pin fins details are mentioned in Table (1). Test base plate section and pin fins arrays (Fig.2) were made of aluminum ( $k_{al} = 200 \text{ W m}^{-1} \text{ K}^{-1}$ ,  $\rho_{al} = 2700 \text{ kg m}^{-3}$ ) because of consideration like cost, machinability, and conductivity. The 17 solids and other

tested pin fins replace on the base test section. A plate heater of approximately the same dimensions as the base test section with the power between (40-120) W heated the lower vertical wall of the base test section to supply a constant heat and base temperature. The amount of heat supplied by the heater is controlled with autotransformer (Variac) and voltage regulator (control interface box). Heat loss to the surrounding from backsides of the heater is minimized by insulating the all duct and test section by glass wool and it is 5% from the amount of heat supplying. In the experiment, the Reynolds number range was 28000-113000, which is based on hydraulic diameter of channel. Air is the working fluid in the experiment. The air temperature for after and before test section heat sink sides measures by K-thermocouples. Each run of experiments take 35 min even after the steady-state which is between 55-60 min after that, more than seventy reading for various pin fin surfaces have been measured and recorded to calculate the average surface temperature using thermal imaging infrared camera (FLIR E30). The pressure drop across the test heat sink section (due to the flow through the pin fins assembly) was measured using Dwyer 475-1-FM-AV. two static pressure Pitot tube/ tapings fixed at the top and the bottom of the test heat sink section, in which the tapings are away 100 mm from the up and down stream of the test heat sink section. All the above equipments used for various measurements were calibrated.

### Data processing and analysis

The heat transfer mode in the present work is conduction, convection, radiation through the air. The magnitude of each mode depends on the temperature of pin fin array base, the geometry and the flow rate .Steady state heat transfer from pin fin array base is:

$$Q_{convection} = Q_{total} - Q_{loss} \quad (1)$$

Where  $Q_{conv}$  is Heat convection through the pin fin array and the steady state heat transfer from pin fin array base  $Q_{total}$  is equal of electrical heat input and calculated from the electrical potential and current supplied to the pin fin array base. The total radiative heat losses from the test section would be about 0.5 % of total electric heat input (Naik et al. 1987, Hwang et al. 1995 and Sara 2001). Therefore, the radiative heat loss can be neglected. The conductive heat loss through the back sidewall of pin fin base array is measured and it is about 3% of the amount of the electrical heat input.

The heat transfer by convection from the surface of pin fin array with including base plate is given by Newton's law of cooling:

$$Q_{convection} = h_{av} A_s \left[ T_{s,av} - \left( \frac{T_{out} + T_{in}}{2} \right) \right] \quad (2)$$

Hence average convective heat transfer coefficient  $h_{av}$ , can be find out as:

$$h_{av} = \frac{Q_{convection}}{A_s \left[ T_{s,av} - \left( \frac{T_{out} + T_{in}}{2} \right) \right]} \quad (3)$$

Where  $T_{out}$  and  $T_{in}$  are the mean temperatures of the air flow at the outlet and the inlet, respectively, were determined by the averaging of the three k-type thermocouples measured at the downstream of test section and three k-type thermocouples at the upstream of the test section . section.  $T_{s,av}$  is the average pin fin array test section surface temperature

measured and recorded by using thermal imaging infrared camera (FLIR E30).  $A_s$  is the surface area of pin fin array including the base of test section and can be expressed on the following equations (all the parameters below is mentioned in table :

$$A_s = b^2 + \pi d H N + N_p (\pi d_{Hp} d + \pi d_{Lp} d) N + \pi d_{Vp} H N - \left(\frac{\pi}{4}\right) d^2 N \quad (4)$$

Where  $b$ ,  $d$ ,  $H$ ,  $N$ ,  $N_p$ ,  $d_{Hp}$ ,  $d_{Lp}$  and  $d_{Vp}$  are base length, diameter of pin fin, pin fin number, perforation number, diameter of horizontal perforation, diameter of lateral perforation and diameter of vertical perforation respectively.

The dimensionless groups, duct Nusselt number  $Nu$  and duct Reynolds number  $Re$  are calculated as follows:

$$Nu = \frac{h_{sk} d_h}{K_{air}} \quad (5)$$

$$Re = \frac{\rho_{air} V d_h}{\mu_{air}} \quad (6)$$

Where  $d_h$ ,  $K_{air}$ ,  $\rho_{air}$  and  $\mu_{air}$  are hydraulic diameter for channel, thermal conductivity, density and viscosity for air respectively. The pressure drops over the test section in the model were measured. The pressure drop can be arranged in dimensionless form by using the following relation:

$$f = \frac{\Delta P}{\frac{\rho_{air} V^3 d_h}{2 P_{in} P_{out}}} \quad (7)$$

Here  $\Delta P$  is the pressure drop of the airflow across the test pin fin array,  $V$  is the mean input channel velocity over the channel cross section.  $\Delta P$  can expressed as:

$$\Delta P = P_{in} - P_{out} \quad (8)$$

#

Where  $P_{in}$  and  $P_{out}$  inlet and outlet pressure respectively. The related thermo physical properties of the working fluid are obtained using the bulk mean temperature, which is (Foo et al. 2012, Tahat et al. 2000, Naik et al. 1987, Hwang et al. 1995 and Sara 2001)

$$T_m = \frac{(T_{in} + T_{out})}{2} \quad (9)$$

In the present study, define the overall thermal efficiency  $\eta$  as follows; (Foo et al. 2012)

$$\eta = \frac{Nu}{\Delta P} \quad (10)$$

Overall thermal efficiency is described the relative pumping power (pressure drop) to achieve a certain rate of heat transfer .

## RESULTS AND DISCUSSION:

Based on the FLIR thermal imaging measurement it was determined after steady state that the maximum, minimum and average temperature of the monitored box area was various as shown in figure 3. The boundary conditions for all images in figure 3 are 3 m/s input velocity, 100 W input power and 18 °C inlet air temperature. It is clearly shown that the maximum, minimum and average temperature for box area is lowered for HV and HLV perforations pin fin arrays than that the solid pin fin arrays. In addition, the temperature distribution bar for three thermal images in figure 3 at the right hand side gives a clear impression for perforations effectiveness. Finally, temperature drop from fin base to fin top surface increases with addition of lateral perforations (Shaeri and Yaghoubi 2009).

Figure 4 shows the pin fin array Nusselt number as a function of Reynolds number for solid, horizontal/vertical (HV) perforations and horizontal/lateral/vertical (HLV) perforation considered in the present work. It is clearly that the perforations have influence on the rate of average heat transfer. Adding 5 lateral perforations to the pin fin array increases the surface area in direct contact with working fluid. The results of the HLV perforations are found good enhancement from HV perforations and from the solid pin fin array. In figure 5 it is clearly shown that the friction factor for the duct with solid pin fins array is higher than that for HV and HLV pin fin array and also substantially higher than that for the smooth duct. Solid pin fin array presents a higher-pressure drop of the airflow across the test pin fin array than HV and HLV perforated pin fins. The results for HLV perforated pin fin array friction factor are found good effectively. Figure 6 shows the variation of the overall thermal efficiency for solid, HV and HLV perforated pin fin arrays. It is clearly shown that the HLV perforated pin fin array has a higher overall thermal efficiency than that solid and HV perforated pin fin array. This can be attributed to the fact that the HLV perforated pin fin array has a higher contact surface area with the working fluid than that in solid and HV pin fin array (high thermal dissipation) and lower pressure drop relative to that in solid pin fin array.

The average Nusselt number and friction factor for the staggered perforated array of pins like fins were correlated as a function of Reynolds number and Prandtl number by using LAB Fit program and the following expressions were obtained:

For solid pins like fins:

$$Nu = 11.05Re^{0.3521} Pr^{0.9088} \quad (11)$$

$$f = 0.36161Re^{-0.0964891} \quad (12)$$

For horizontal /vertical (HV) perforations;

$$Nu = 22.04Re^{0.2787} Pr^{0.1281} \quad (13)$$

$$f = 0.0924531Re^{-0.02255127} \quad (14)$$

And for horizontal/vertical/lateral (HVL) perforations;

$$Nu = 21.350154Re^{0.3049} Pr^{0.72021} \quad (15)$$

$$f = 0.1573651Re^{-0.06817} \quad (16)$$

One of the performance evaluation criterions (sparrow 1980, Sara 2003) is to compare the heat transfer coefficient for constant pumping power for the channel with finned surface with that for the smooth surface. The pumping power is proportional to  $f Re^3$ , and the relationship between the finned and smooth duct for the same pumping power is expressed by (Sara 2003):

$$f Re^3 = f_s Re_s^3 \quad (17)$$

Where  $f$  and  $Re$  are the values for the finned duct, and  $f_s$  and  $Re_s$  are those for the smooth duct and the friction factor for smooth channel (without pin fins) was found by Blasius equation as follows;

$$f_s = 0.316 Re^{-0.25} \quad (18)$$

According to the constant pumping power constraint, the mass flow rates (or Reynolds number) passing through the finned and reference smooth channel cannot be the same, since the mass flow rate for the smooth channel must be increased to keep the fluid pumping power constant. Using eq. 11 to expressed  $Re_s$ .

In the present study, define heat transfer enhancement factor,  $Nu^*$ , was used to appraise the possible benefits of using perforation pin fins (Sara 2003):

$$Nu^* = \left( \frac{Nu}{Nu_s} \right)_{\text{equal pumping power}} \quad (19)$$

Where  $Nu_s$  is the average Nusselt number for the smooth channel with  $Re_s$  at which the pumping power is the same as that occurring in the finned channel.  $Nu_s$  can be calculated from the following correlation (Sara et al. 2001)

$$Nu_s = 0.0919 Re_s^{0.706} Pr^{1/3} \quad (20)$$

Figure 7 shows the heat transfer enhancement factor  $Nu^*$  denoted in eq. 13 as a function of equivalent Reynolds number  $Re_s$  for three shapes. It is clearly shown that the HLV perforation shape give a higher heat transfer enhancement factor. Also, all enhancement factors for all shapes are higher than unity. This is an advantage to use a perforation pin fins in the heat transfer enhancement. In addition, for all shapes, the channels with pin fin arrays give higher enhancement factor at lower Reynolds number than those at higher Reynolds number (Sara 2003).

For the constant test section pin fin arrays temperature, fin performance  $\varepsilon_f$  is the ratio of heat transfer from fin to heat transfer from fin base without fin, as fin effectiveness (Shaeri and Yaghoubi 2009 ) and is defined as follows for solid, horizontal/vertical (HV) and horizontal/lateral, vertical (HLV) :

$$\varepsilon_{f,solid} = \frac{h_{av,solid} A_{s,solid} (T_{s,solid} - T_{\infty})}{h_b A_b (T_b - T_{\infty})} \quad (21)$$

$$\varepsilon_{f,HV} = \frac{h_{av,HV} A_{s,HV} (T_{s,HV} - T_{\infty})}{h_b A_b (T_b - T_{\infty})} \quad (22)$$

$$\varepsilon_{f,HLV} = \frac{h_{av,HLV} A_{s,HLV} (T_{s,HLV} - T_{\infty})}{h_b A_b (T_b - T_{\infty})} \quad (23)$$

$$R_{th} = \frac{(T_b - T_{\infty})}{Q_{\text{refinement}}} \quad (24)$$

Where  $T_{\infty}$  is the free stream temperature,  $h_b$  is the fin base average convection heat transfer coefficient,  $A_b$  is the fin base area and  $T_b$  is the base temperature.

The total thermal resistance  $R_{th}$  is primary thermal performance parameter for the pin fin heat sink which is considered in this study as:

$$R_{th} = \frac{(T_b - T_{\infty})}{Q_{\text{refinement}}} \quad (25)$$

$Q_{\text{convection}}$

For constant base section temperature, figure 8 shows the variation of fin effectiveness with Reynolds number for solid, HV and HLV perforated pin fin array. It is clearly shown that for the three types of pin fin arrays, fin effectiveness decreases as Reynolds number increases. In addition, fin effectiveness for HV and HLV perforated pin fin array is higher than for solid pin fin array. Also, for constant base section temperature, figure 9 shows the variation of total thermal resistance with Reynolds number for solid, HV and HLV perforated pin fin arrays. The results show that the thermal resistance of solid pin-fin array is higher than the thermal resistance for HV and HLV perforated pin fin array. This is because the velocity distribution was more disturbances through the HV and HLV perforated pin fin array due to HLV perforation which increases the heat transfer coefficient and decreases the base temperature and decreases the thermal resistance.

Figure 10 shows the present experimental and numerical results comparing with Sara's experimental results for various interfin spacing ratios and clearance ratios. It is clearly shown the same trend for present experimental and numerical results with Sara's results in spite of the different Reynolds number.

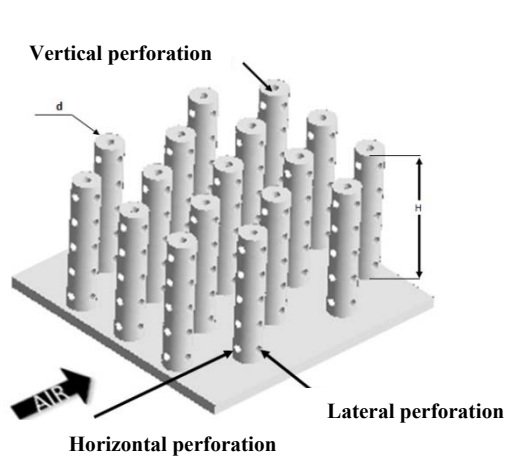
## CONCLUSIONS

In this study, the overall heat transfer, friction factor, thermal efficiency, overall enhancement ratio, fin effectiveness and thermal resistance were investigated experimentally. The effects of the working fluid flow and horizontal/lateral/vertical perforated pin fin array on the overall heat transfer, friction factor, thermal efficiency, overall enhancement ratio, fin effectiveness and thermal resistance were determined. The conclusions are summarized as:

- 1- Average Nusselt number increased with increasing perforations like lateral perforations.
- 2- Friction factor decreased with increasing contact surface area due to perforations.
- 3- HLV perforated pin fin array has a highly thermal dissipated and lower pressure drop relative to solid and HV perforated pin fin arrays
- 4- Maximum overall enhancement ratio is obtained with a minimum value of Reynolds number and it is a higher value for HLV perforated pin fin array.
- 5- The weight reduction for the single HV perforated pin fin is 15.4% relative to that in solid pin fin and the weight reduction for the single HLV pin fin is 21.7% relative to solid pin fin and that mean HLV perforated pin fin is a lighter fins than that solid and HV. HLV perforated pin fin array is achieved in economical.

**Table 1:** Geometric description of the heat sinks tested





| <i>Parameter</i>                              | <i>symbol</i>         | <i>value</i> |
|---|-----------------------|--------------|
| <i>Base length and width</i>                  | <i>b</i>              | 98 mm        |
| <i>Fins number</i>                            | <i>N</i>              | 17           |
| <i>Diameter of the circular pin fin</i>       | <i>d</i>              | 10mm         |
| <i>Height of the circular pin fin</i>         | <i>H</i>              | 50mm         |
| <i>Clearance between the fin and the duct</i> | <i>C</i>              | 12mm         |
| <i>Transversal pitch</i>                      | <i>S<sub>x</sub></i>  | 23mm         |
| <i>Longitudinal pitch</i>                     | <i>S<sub>y</sub></i>  | 21mm         |
| <i>Lateral perforation diameter</i>           | <i>d<sub>lp</sub></i> | 3mm          |
| <i>Horizontal perforation diameter</i>        | <i>d<sub>hp</sub></i> | 3mm          |
| <i>Vertical perforation diameter</i>          | <i>d<sub>vp</sub></i> | 3mm          |
| <i>Duct length</i>                            | <i>L</i>              | 1200mm       |
| <i>Duct cross section width</i>               | <i>w</i>              | 62mm         |
| <i>Duct cross section depth</i>               | <i>l</i>              | 167mm        |
| <i>Perforation number per pin fin</i>         | <i>N<sub>p</sub></i>  | 5            |



Fig. 1a: photographic diagram of the experimental rig.

| Item | Description                             |
|------|---|
| ١    | Mouth                                   |
| ٢    | Flow straightner                        |
| ٣    | Inlet Pitot tube(Pressure in)           |
| ٤    | Inlet temp. thermocouple(T in)          |
| ٥    | Insulated duct                          |
| ٦    | Heat sink insulation                    |
| ٧    | Heater (constant heat flux)             |
| ٨    | Heat sink base T ave thermocouples      |
| ٩    | Heat sink insulated base                |
| ١٠   | Outlet Pitot tube( Pressure out)        |
| ١١   | Outlet temp. thermocouple(T out)        |
| ١٢   | differential manometer Digital          |
| ١٣   | Control interface box                   |
| ١٤   | Computer                                |
| ١٥   | Variable speed blower control           |
| ١٦   | Test section (pin fin array heat sink)) |

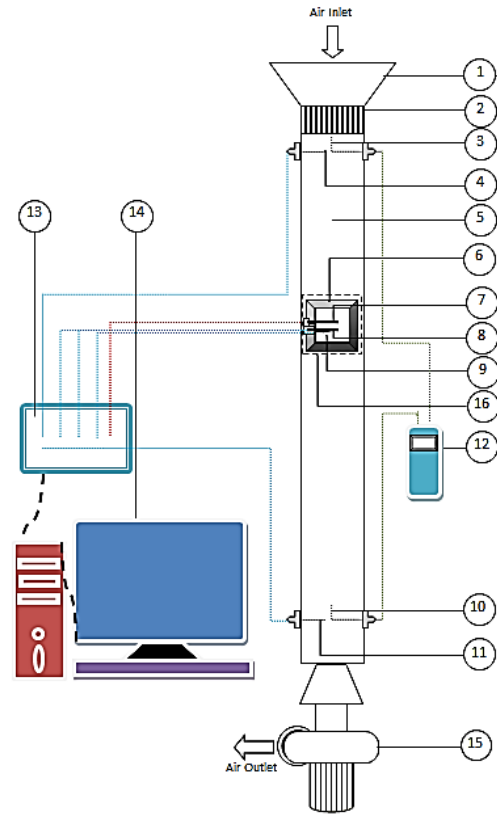
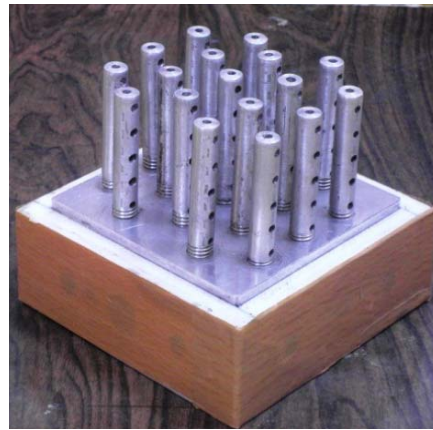


**Fig. 1b:** Schematic diagram of the experimental rig.



(a)



(b)



(c)

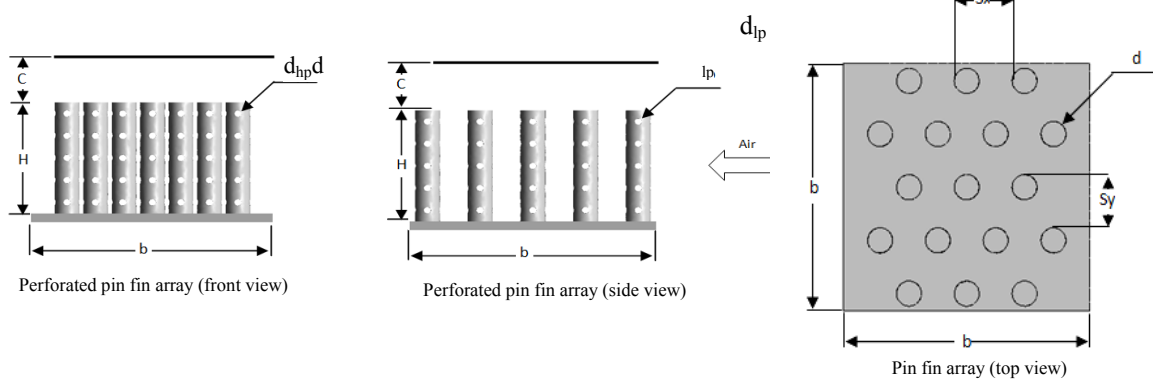
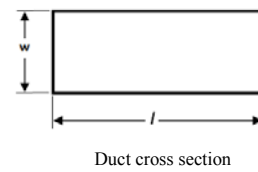


**Fig. 2:** (a) solid pin fin array , (b) pin fin array with horizontal / vertical(HV) Perforations and (c) pin fin arrays with horizontal / lateral / vertical (HLV)

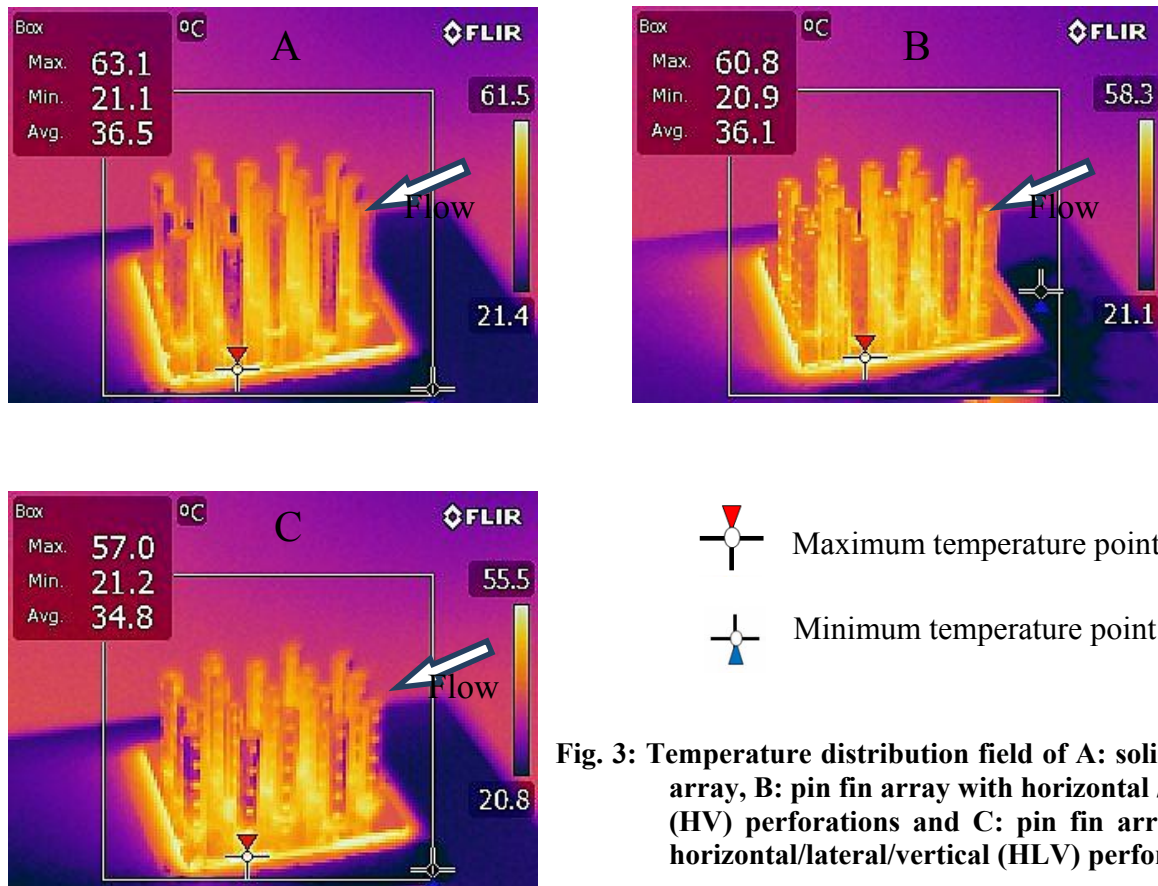


Fig. 3: Temperature distribution field of A: solid pin fin array, B: pin fin array with horizontal / vertical (HV) perforations and C: pin fin arrays with horizontal/lateral/vertical (HLV) perforations.

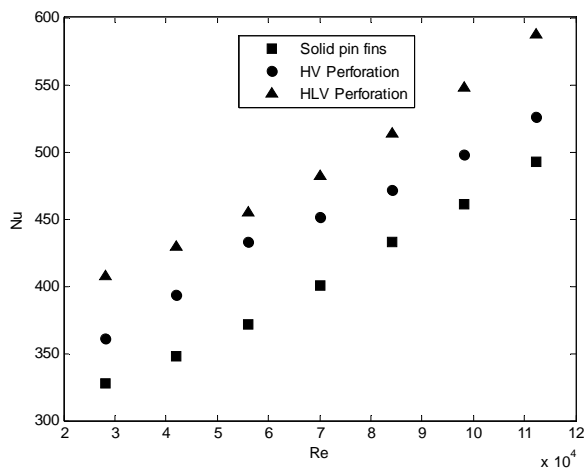


Fig. 4: Variation of Nusselt number with Re for solid pin fin, HV perforation and HLV perforation.

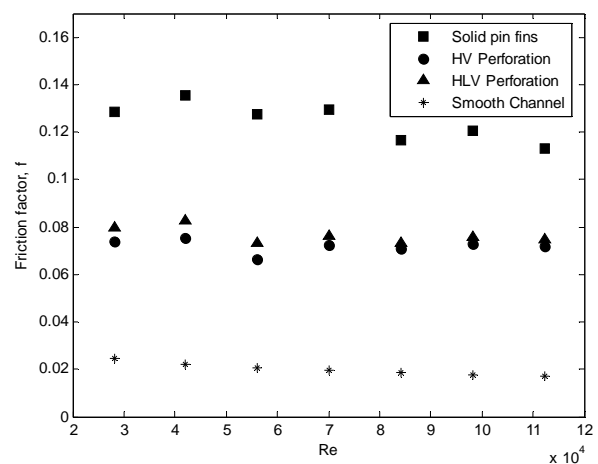


Fig. 5: Variation of duct friction factor with Re for solid pin fin, HV perforation and HLV perforation.

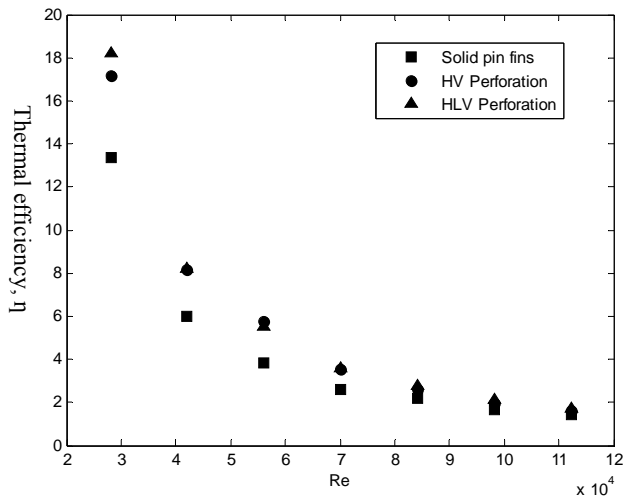


Fig.6: Variation of thermal efficiency with  $Re$  for solid pin fin, HV perforation and HLV perforation.

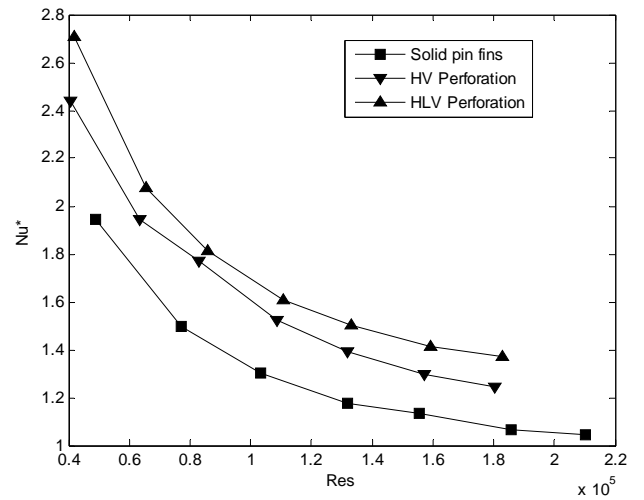


Fig. 7: Heat transfer enhancement factor as a function of equivalent Reynolds number for three shapes.

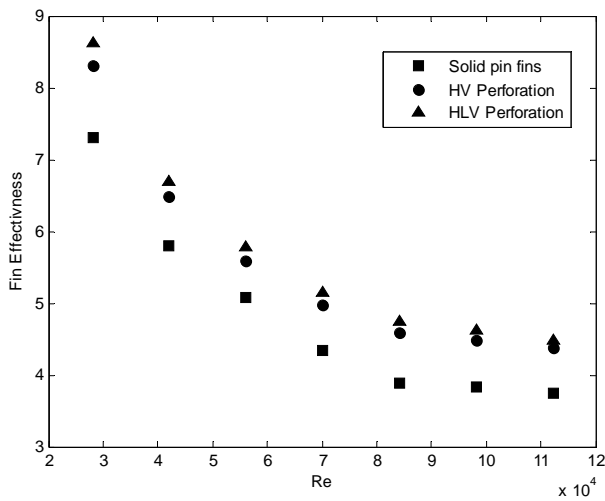


Fig. 8: Variation of fin effectiveness with  $Re$  for solid pin fin, HV perforation and HLV perforation.

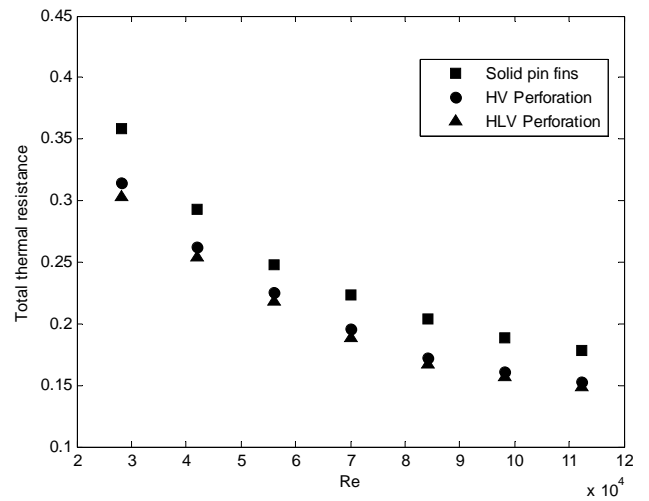
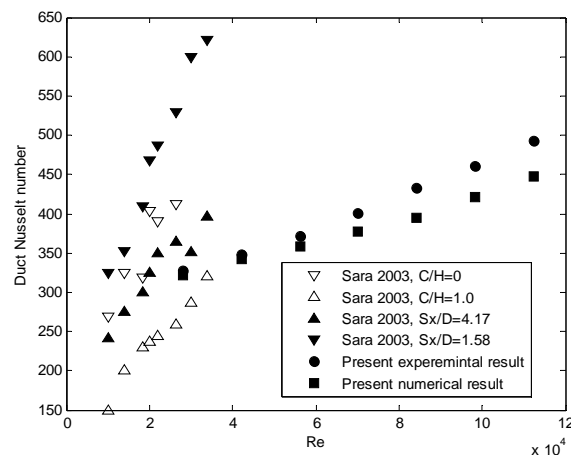


Fig.9: Variation of total thermal resistance with  $Re$  for solid pin fin, HV perforation and HLV perforation.



**Fig.10: Duct Nusselt number vs. Reynolds number for present experimental and numerical results with various interfin spacing ratio and clearance ratio for Sara 2003.**

## REFERENCES :-

Andrea Diani, Simone Mancin\*, Claudio Zilio, Luisa Rossetto, An assessment on air forced convection on extended surfaces: Experimental results and numerical modeling, *International Journal of Thermal Sciences* 67 (2013) 120-134.

Bayram Sahin, Alparslan Demir, Performance analysis of a heat exchanger having perforated square fins, *Applied Thermal Engineering* 28 (2008) 621-632.

E. M. Sparrow, J. W. Ramsey, C. A. C. Altemani, Experiments on in-line pin fin arrays and performance comparison with staggered arrays, *Trans. ASME J. Heat transfer* 102 (1980) 44-50.

Hwang JJ, Liou TM. Heat transfer and friction in a low-aspect-ratio rectangular channel with staggered perforated ribs on two opposite walls. *ASME J Heat Transfer* 1995;117(11):843–50.

Ji-Jinn Foo, Shung-Yuh Pui, Yin-Ling Lai, Swee-Boom Chin, Forced convective heat transfer enhancement with perforated pin fins subject to an impinging flow, *SEGi Review* ISSN 1985-5672 Vol. 5, No.1, (July 2012) 29-40.

Kai-Shing Yang, Wei-Hsin Chu, Ing-Yong Chen, Chi-Chuan Wang, A comparative study of the airside performance of heat sinks having pin fin configurations, *International Journal of Heat and Mass Transfer* 50 (2007) 4661-4667.

M. R. Shaeri, M. Yaghoubi, Numerical analysis of turbulent convection heat transfer from an array of perforated fins, *International Journal of Heat and Fluid Flow* 30 (2009) 218-228.

M.R. Shaeri, M. Yaghoubi \*, K. Jafarpur, Heat transfer analysis of lateral perforated fin heat sinks, *Applied Energy* 86 (2009) 2019–2029.

M. Tahat, Z.H. Kodah, B.A. Jarrar, S.D. Probert, Heat transfer from pin fin arrays experiencing forced convection, *App. Energ.* 67 (2000) 419-442.

Naik S, Probert SD, Shilston MJ. Forced convective steady-state heat transfers from shrouded vertical fin arrays aligned parallel to an undisturbed air-stream. *Appl Energy* 1987;26:137–58.

Sara ON, Yapıcı S, Yılmaz M, Pekdemir T., Second law analysis of rectangular channels with square pin-fins, *Int. J. Commun. Heat Mass Transfer* 2001;28(5):617–30.

Sara ON, Performance analysis of rectangular ducts with staggered square pin fins, *Energy Conversion and Management* 44 (2003) 1787–1803.

Tzer-Ming Jeng, Sheng-Chung Tzeg, A semi-empirical model for estimating permeability and inertial coefficient of pin-fin heat sinks, *International Journal of Heat and Mass Transfer*, 48 (2005) 3140-3150.

Yu Rao a, Chaoyi Wana, and Yamin Xu, An experimental study of pressure loss and heat transfer in the pin fin-dimple channels with various dimple depths, *International Journal of Heat and Mass Transfer* 55 (2012) 6723–6733.